Synthesis, Activity, and Molecular Modeling of New 2,4-Dioxo-5-(naphthylmethylene)-3-thiazolidineacetic Acids and 2-Thioxo Analogues as Potent Aldose Reductase Inhibitors

Patrick Fresneau,[†] Max Cussac,*[,†] Jean-Marc Morand,[†] Barbara Szymonski,[†] Duc Tranqui,[§] and Gérard Leclerc[‡]

Laboratoire de Chimie Thérapeutique and Laboratoire de Chimie Organique, Groupe de Pharmacochimie Moléculaire, EP811-CNRS, UFR de Pharmacie, Université Joseph Fourier de Grenoble, Domaine de la Merci, 38700 La Tronche, France, and Laboratoire de Cristallographie, UPR 5031-CNRS, Avenue des Martyrs, 38042 Grenoble Cedex, France

Received March 6, 1998

A series of 2,4-dioxo-5-(2-naphthylmethylene)-3-thiazolidineacetic acids and 2-thioxo analogues have been prepared as aldose reductase inhibitors. In vitro inhibitory activities of bovine lens aldose reductase were determined by a conventional method. 1-Naphthyl-substituted derivatives of the 2-thioxo series were the more potent inhibitors ($IC_{50} \cong 10$ nM) with similar activity to that of Epalrestat. Structural analysis, especially by X-ray crystallography of two selected compounds, and molecular modeling comparisons with Zopolrestat were performed. These results provide explanations of the good activity of the inhibitor, the preference for 1-naphthyl-substituted compounds, and the nature of molecular interactions in these systems.

Introduction

Progression of chronic diabetes results in long-term, debilitating complications such as cataractogenesis and microangiopathy including nephropathy, retinopathy, and neuropathy thought to be linked to excess free glucose in corresponding tissues and leading to increased flux of glucose through the polyol pathway.[1,2] Numerous observations have provided evidence of aldose reductase (AR) implication in diabetic complications.[3−11] Inhibition of aldose reductase, the first enzyme of the polyol pathway, is therefore a useful strategy for prevention and treatment of complications of chronic diabetes. A considerable effort in this search has led to the discovery of a large number of AR inhibitors.[12−18]

Looking at specific structural and electronic similarities of apparently diverse AR inhibitors, it appears that they can be divided into four main classes of structures, all having an acidic character: carboxylic acids, phenolic compounds, those containing an amide or imide or carbamate or sulfonamide group with an acidic hydrogen on the nitrogen atom, and those containing an activated hydrogen on the carbon atom. Structural requirements for activity were established by Kador et al., and these consist of a generally planar structure with two hydrophobic (aromatic) regions and a substructure susceptible to charge-transfer interactions.[15,19]

Therefore, in view of our study of 5-(arylmethylene)-2-thiohydantoin derivatives as immunomodulators[20] and by analogy with a potent known AR inhibitor, Epalrestat, we synthesized heterocyclic related compounds with structural variations on the aromatic moiety and determined their AR inhibitory potency using a classical in vitro biological assay. Having found especially good results (IC_{50} values ranging from 10 to 100 nM for compounds of the 2-thioxo series) we tried to explain their noteworthy activity and their differential potency by performing a molecular modeling study of two of our best compounds well-characterized by experimental NMR and crystallographic structural data and by comparing the results to those obtained for Zopolrestat. This study was facilitated by recent publications relating to the crystallographic structure of aldose reductase.[21−25]

Scheme 1. General Preparation of Titled Compounds

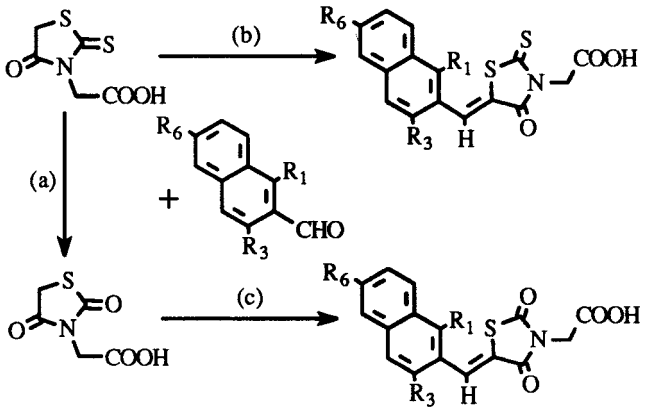

Chemistry

The preparation of 2,4-dioxo-5-(2-naphthylmethylene)-3-thiazolidineacetic acids (2-oxo derivatives) and of 4-oxo-2-thioxo-5-(2-naphthylmethylene)-3-thiazolidineacetic acids (2-thioxo derivatives) involved the condensation, according to Knoevenagel, of 2,4-dioxothiazolidine-3-acetic acid or its 2-thioxo analogue (rhodanineacetic acid) with appropriate 2-naphthaldehydes (Scheme 1).

The derivatives of the 2-thioxo series are usually more reactive than the 2-oxo derivatives. The reactivity also depends on the type of substituent on the naphthalene ring. Bromine, chlorine, and methoxy groups are usu-

[†] Laboratoire de Chimie Thérapeutique.
[‡] Laboratoire de Chimie Organique.
[§] Laboratoire de Cristallographie.

10.1021/jm9801399 CCC: $15.00
Published on Web 10/28/1998

Scheme 2

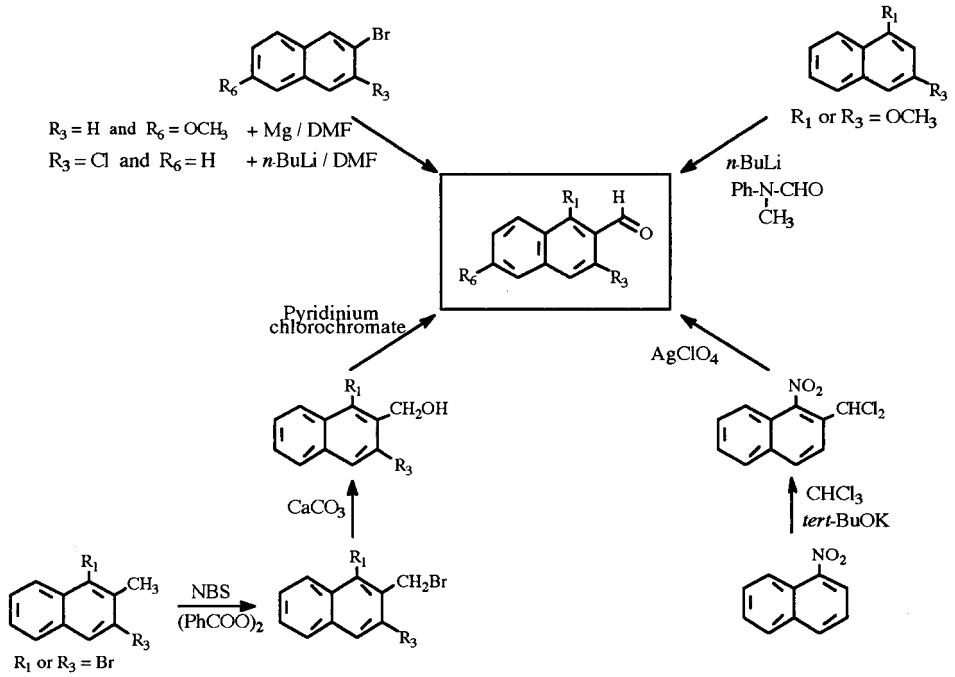

ally activating at all positions, whereas the 1-nitro group is activating in the 2-thioxo series but disactivating in the 2-oxo series.

The substituted naphthaldehydes were usually obtained by the introduction of the formyl group on the naphthalene ring bearing the appropriate substituent according to four different methods (Scheme 2): (1) From the reaction of DMF with the Grignard reagent derived from 6-methoxy-2-bromonaphthalene as described by Eriguchi et al.[26] or with the organolithium derivative of 2-bromo-3-chloronaphthalene. The synthesis of this intermediate from 2-bromoindene, according to Lindley et al.,[27] involves enlarging the ring size followed by a chlorination step using chloroform. (2) From the reaction of *N*-methylformanilide with the organolithium derivatives of 1-methoxynaphthalene and 3-methoxynaphthalene. (3) From the reaction of chloroform with 1-nitronaphthalene in the presence of *t*-BuOK, by modification of the Riemer−Tiemann reaction where the hydrolysis of the *gem*-dichlorinated intermediate occurs in the presence of silver perchlorate as described by Makosza et al.[28] (4) By the oxidation of methyl groups of 1-bromo-2-methylnaphthalene and 3-bromo-2-methylnaphthalene. The methyl group was subjected to bromination by NBS, the resulting bromo derivative was subsequently hydrolyzed, and the primary alcohol was then oxidized using pyridinium chlorochromate as described by Corey et al.[29] 1-Bromo-2-methylnaphthalene was synthesized by bromination according to Adams et al.[30] 3-Bromo-2-methylnaphthalene was prepared by modification of Danish's method for the synthesis of 2-methyl-3-bromonaphthalene[31] which involves a pyrolysis reaction of 3-bromohexachlorocyclopentadiene adduct of 2-methyl-3-bromonaphthalene.

Structural Analysis

^{1}H NMR and ^{13}C NMR spectroscopy were used to determine the structure of all listed compounds, in particular the conformation of the exocyclic double bond.[32] One-dimensional ^{1}H NMR and ^{13}C NMR as well as two-dimensional homonuclear or heteronuclear NMR were required to interpret the spectra. This was based partly on work by Katrisky et al.[33] on the analysis ^{1}H NMR spectra of naphthalenes which are generally complicated due to the overlapping of signals which are strongly coupled together and partly on work by Breitmaeir et al.[34] on the analysis of ^{13}C NMR spectra. The exocyclic double bond of all compounds adopts a *Z*-configuration as determined by the anisotropic effect exerted by the carbonyl (C_4=O) group on the H-3 proton of the naphthalene ring. This was confirmed by the coupling constant value of the vicinal carbons in ^{13}C-coupled spectra as shown by Vögeli et al.[35] and Ishida et al.[36] The variations observed in the *J* values of our compounds (5.52−7.21 Hz) are characteristic of a *Z*-configuration. X-ray crystallographic data from compounds **1** and **2** indicate these also adopt a *Z*-configuration.[37]

Pharmacology

In vivo studies on the inhibitory effect of compounds **1**−**16** on AR activity were carried out on an extract of beef crystalline enzyme according to the method of Kador and Sharpless.[38] The percentage inhibition was determined by UV spectrophotometry from the lowering in enzyme activity measured by the diminution of the enzymatic reduction of D-glyceraldehyde in the presence of NADPH and an inhibitor. The in vitro inhibitory concentrations (IC_{50}) were then calculated from the graph and are shown in Table 1.

Studies on the level of enzyme activity were carried out using Ponalrestat as a control (IC_{50} = 7 nM for conditions of the experiment). It is noteworthy to point out that literature values indicate an in vitro activity which is comparable: 7.7 nM[39] and 26 nM.[40] A comparison of the in vitro inhibition constant values of other well-known inhibitors [Zopolrestat = 3 nM (human placenta);[41] Epalrestat = 10 nM (rat crystalline);[42]

Table 1. In Vitro IC_{50} Values (nM) of Aldose Reductase Inhibition

formula	compd	X	R_1	R_3	R_6	IC_{50} (nM)
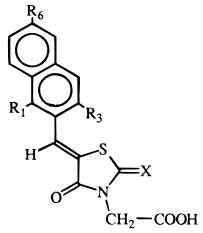	**1**	S	H	H	H	96
	2	S	OCH_3	H	H	9
	3	S	Br	H	H	11
	4	S	NO_2	H	H	79
	5	S	H	OCH_3	H	20
	6	S	H	Br	H	15
	8	S	H	H	OCH_3	67
	9	O	H	H	H	269
	10	O	OCH_3	H	H	150
	11	O	Br	H	H	51
	13	O	H	OCH_3	H	128
	14	O	H	Br	H	153
	15	O	H	Cl	H	48
	16	O	H	H	OCH_3	101
Ponalrestat 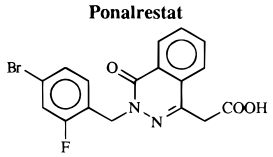						7 7.7 (lit.[39]) 26 (lit.[40])

Tolrestat = 35 nM (veal crystalline);[43] *S*-(+)-Sorbinil = 150 nM (beef crystalline)[44]] with those of our compounds (Table 1) indicates that the latter are good inhibitors of aldose reductase activity.

Discussion and Molecular Modeling

The activity results shown in Table 1 indicate that the 2-thioxo derivatives are more active (IC_{50} range 9−96 nM) than the 2-oxo analogues (IC_{50} range 48−269 nM), an increase in lipophilic character leads to greater activity (**10**−**16** vs **9**; **2**−**8** vs **1**), and in three cases out of four there is increased, although modest, inhibitory activity observed for naphthalene derivatives substituted at the 1-position rather than at the 3-position (**2** vs **5**, **3** vs **6**, or **11** vs **14**). However the IC_{50} values obtained do not allow us to conclude the best position of the substitution between the 1- and 6-position (**2** > **8** but **10** < **16**). Finally the electron-donating OCH_3 substituent is more favorable than the electron-withdrawing Br and even more so with NO_2 (**2** > **3** ≫ **4**).

Molecular modeling studies were carried out in order to explain the disparity between the activity of some of the products. We wished to examine, at the molecular level, the interaction between aldose reductase and several compounds, namely, the nonsubstituted inhibitor **1** (IC_{50} = 96 nM) and the substituted inhibitor **2** (IC_{50} = 9 nM) which exhibits the best inhibitory activity of all compounds.

Our study has benefited from recent results of X-ray studies of AR[21−23] and of AR complexed with substrates or inhibitors.[24,25,45] This work began after publication of the AR·$NADP^+$·glucose-6-phosphate ternary complex by Harrison et al.[25] and used his coordinates deposited in the Protein Data Bank (code 1ACQ). We tried first to retrieve Wilson's published crystallographic results of the AR·Zolporestat complex[24] despite the initial embargo of the coordinates for this structure, and we applied this knowledge to our inhibitors **1** and **2**.

Construction of Models of the AR·Inhibitor Complex. To study the interaction of an inhibitor with the enzyme in the complex, it must be taken into account that the number of different ways of putting the molecules together is very large. We proposed, within Sybyl,[46] a computerized manual docking procedure, a variety of positions of the inhibitor in the active site of AR, whose validity was checked by energy minimization of the proposed complex until distances and angles were physically acceptable and until convergence to the lowest-energy values.

Our 3D-models for the AR·inhibitor complex construction were achieved using the following assumptions:

(1) Starting conformations of inhibitors were taken from minimized anionic structures resulting from a conformational analysis by a grid search procedure run with crystallographic structures of inhibitors **1** and **2** or with a built structure of Zopolrestat. It is not the sole way to reach likely conformations, but it is a reliable one which provided, in addition, a good evaluation of the acceptable torsional angle variations around rotatable bonds, i.e., those compatible with energy levels within a chosen 3 kcal/mol range of the lowest one.

(2) To build models consistent with mutational data, inhibitors were docked to form a hydrogen-bonding interaction between one oxygen of the carboxylate group of the inhibitor and the OH group of Tyr48. This group is important for AR activity because its mutation to phenylalanine (Y48F) cancels the enzymatic activity.[47−49] It has also been proposed as a proton-donor group for the reductase activity in the catalytic mechanism.[22,25,47,49] Moreover, the oxygen of the carboxylate group must be close to $N_{\epsilon 2}$ of His110 which directs substrate stereochemical selectivity in the enzymatic reduction reaction as shown by mutagenesis substitution.[48] Finally the carboxylate carbon of the inhibitor, which could be considered analogous to the substrate's carbonyl carbon, must lie within a favorable distance of the nicotinamide C_4 carbon from which the transferring hydride originates. So the oxygen of the carboxylate group must be located in the plane described by the phenolic hydroxyl of Tyr48, the $N_{\epsilon 2}$ of His110, and the C_4 carbon of the nicotinamide ring which was proposed as the common binding site for substrates and anionic inhibitors.[25]

(3) The possibility of making a hydrogen-bonding interaction with the thiol group of Cys298 was taken into account because its mutation to Ser (C298S) altered kinetic parameters of AR and markedly reduced sensi-

Table 2. Important Intermolecular Distances (Å) in AR·Inhibitor Complexes

	inhibitor										
	Zopolrestat								citrate		
	Wilson's study			our modeling					Harrison's study		
aldose reductase	CO*O*$^-$	*C*OO$^-$	*C*OO$^-$	CO*O*$^-$	*C*OO$^-$	*C*OO$^-$	BtC_8[a]	BtC_9[a]	CO*O*$^-$	*C*OO$^-$	*C*OO$^-$
Tyr48-*O*	2.65	≫2.89		2.68	4.41	3.76			3.37	3.51	3.86
His110-Nϵ_2	2.89	≫2.89		3.50	3.22	3.69			2.78	4.67	3.87
nicotinamide C_4			3.63	3.14	3.93	3.31			3.19	3.75	3.63
Leu300-Cγ							4.05	3.32			
W111-C_8							2.97	3.15			
W111-C_9							3.21	3.24			

[a] Bt, benzothiazole.

bility of AR to inhibition by Sorbinil[23,49] and because its chemical alkylation showed similar effects.[50]

(4) On account of the too large size of certain acidic inhibitors, such as Zopolrestat and other flexible inhibitors with two aromatic ring systems, whose structure cannot be totally accommodated by the elliptical active site pocket of AR, we were compelled to seek hydrophobic interactions of the second aromatic ring system (remote from the carboxylate group) with amino acids of the wall of the active site pocket especially with Trp111 as described in Wilson's crystallographic study of the AR·Zopolrestat complex.[24] So we placed the benzenic ring of the benzothiazole moiety of Zopolrestat into the groove between Trp111 and Leu300. In the case of inhibitors **1** and **2**, the naphthyl moiety was placed into this groove.

(5) For the AR·Zopolrestat complex, we positioned the inhibitor so that an extra hydrogen bond could be made between the CF_3 moiety of Zopolrestat and the OH group of Thr113, as mentioned in Wilson's results.

(6) To optimize bonding geometries and to relieve close van der Waals contacts, adjustments were made in the side-chain conformation of Leu300, in conformations of the inhibitor, and in ligand positions. The side chain of Leu300 was moved away slightly to facilitate positioning of the benzothiazole or naphthyl moiety of the inhibitor between Trp111 and Leu300, and torsional angle values of the rotatable bonds were modified within an energy loss of $\Delta E < 3$ kcal/mol, consistent with the Gridsearch results, to accommodate the inhibitor molecule and facilitate bonding contacts.

After the inhibitor was positioned within AR, the resulting conformation was subjected to an automatic docking according to the Powell method[51] using the Tripos force field. According to the Anneal function in Sybyl,[46] this minimization was restricted to all atoms of the inhibitor and those AR atoms located at a distance = 10 Å from the inhibitor molecule (hot region). This minimization also took into account the electronic effects of those AR atoms located between 10 and 15 Å (interesting region), but their position was kept fixed. A dielectric constant value of 3.5 was chosen due to the high hydrophobic character of the active site pocket of AR. Indeed six aromatic residues (Trp20, Trp79, Trp111, Phe115, Phe122, and Trp219), three nonpolar residues (Ala299, Leu300, and Pro310), and four polar residues (Tyr48, His110, Cys298, and Tyr309) were originally found lining the active site pocket.[22] This hydrophobic feature is consistent with the high-affinity binding of hydrophobic substrates as aromatic aldehydes[52] and steroids[53] and of some AR inhibitors. Various positions and minimizations were performed. A tendency toward a common low-energy geometry supports the proposed model for the AR·inhibitor complex.

The AR·Zopolrestat Complex. The bound Zopolrestat occupies the entire active site pocket and makes an unusually large number of contacts with surrounding amino acid side chains (Figure 1). Major determinants of the interaction are hydrogen bonds having distances between 2.8 and 3.3 Å, the first two being very strong [CO*O* from Tyr48-*O*H = 2.68 Å, angle = 159°; C*F* from Thr113-*O*H = 2.74 Å, angle = 139°; N_2 (phthalazinone moiety) from Cys298-*S*H = 3.27 Å, angle = 115°].

Other important features are the numerous tight hydrophobic interactions, especially those keeping the benzothiazole moiety between Trp111 and Leu300 (distances from Trp111 ranging from 3.0 to 3.3 Å and from Leu300 ranging from 3.3 to 4.1 Å). The phthalazinone ring is sandwiched between Phe122 and Trp20 but with more room (shortest distances from Phe122 = 4.15 Å and from Trp20 = 3.60 Å). The inhibitor's carboxylate group and the side chain of His110 are in close contact (C*O*O to His110-N_2 = 3.22 Å), and its carboxylate carbon is within a very favorable distance (3.31 Å) of the nicotinamide C_4 carbon from which the transferring hydride originates. These important features of the binding make Zopolrestat a very potent inhibitor of AR.

These results are very similar to those of Wilson's crystallographic study of the AR·Zopolrestat complex and they agree also with Harrison's crystallographic study of the AR·citrate complex as seen in Table 2. The only minor differences with Wilson's report are the position of the O_2 carbon of the carboxylate group. In our model the O_3 atom of the carboxylate group (CO*O*) makes a strong hydrogen bond with Tyr48-*O*H (2.68 Å), as in Wilson's study, but none with the N_2 atom of His110. In addition, the O_2 atom of the carboxylate group (C*O*O) is nearer His110-N_2 (3.22 Å) than the O_3 atom, while Wilson reported the O_3 atom is involved in a shared hydrogen bond with Tyr48-*O*H (2.65 Å) and with His110-N_2H (2.89 Å). A likely reason is the fact that we used the AR·glucose-6-phosphate 3D-structure from the PDB database as a starting enzyme structure. This complex does not bear an H atom at the His110-N_2 site, while Wilson's study used the acidic molecule of Zopolrestat which was crystallized in the enzyme making a salt link involving carboxylate group and cationic His110-N_2H^+.

The AR·Inhibitor 1 Complex. As observed with Zopolrestat, the inhibitor **1** molecule occupies the entire active site pocket with numerous contacts with surrounding amino acid side chains (Figure 2). The more

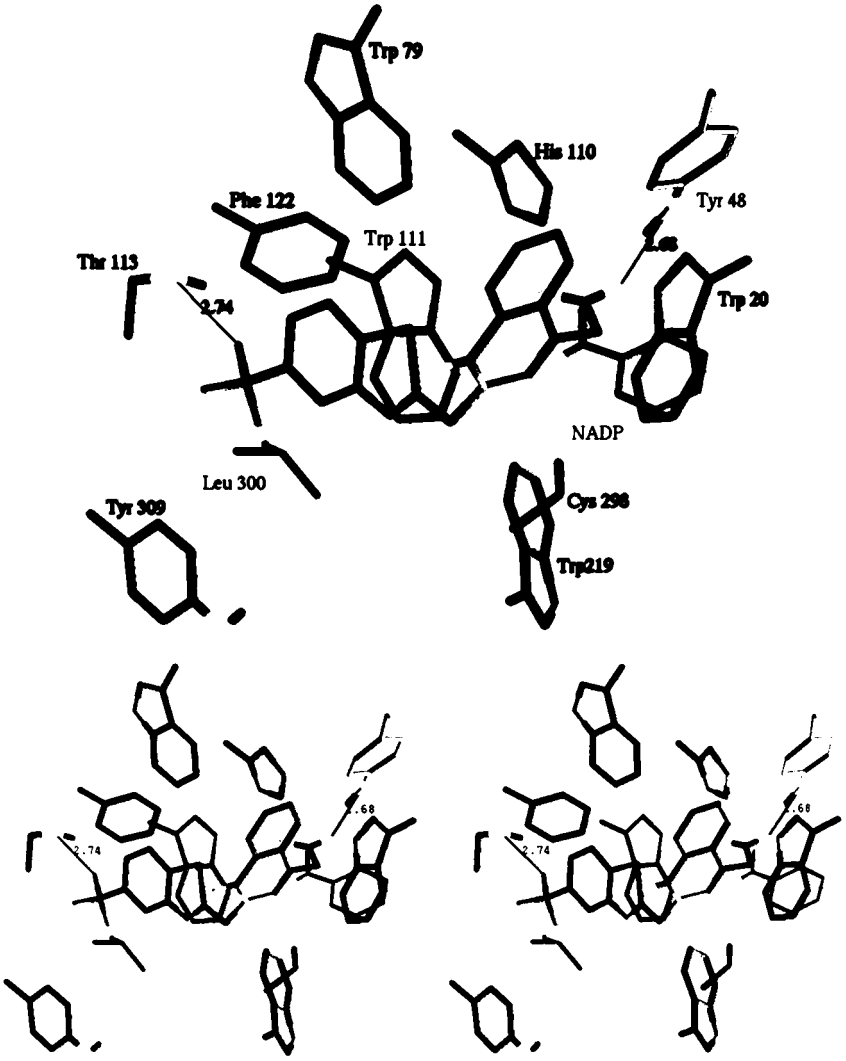

Figure 1. Zopolrestat docked into the aldose reductase binding pocket. Carbon atoms of Zopolrestat and those of the surrounding AR side-chain amino acids are shown in black except those of the nicotinamide moiety (under Trp20) and those, poorly illuminated, of Tyr48 (carbons β, 2, 5). Heteroatoms are gray. Only H atoms likely to make H-bonds are shown in black. The two strong H-bonds with HO-Tyr48 = 2.68 Å and with HO-Thr113 = 2.74 Å are shown (thin lines). (Top) Detailed view of AR·Zopolrestat interaction with labeled amino acids. (Bottom) Stereoview of AR·Zopolrestat interaction.

important features of the interaction are the hydrogen bond between the carboxylate group and the hydroxyl of Tyr48 [d(COO^- from Tyr48-OH) = 3.08 Å, angle = 160°] and the tight hydrophobic interactions which keep the naphthyl ring between Trp111 and Leu300 (distances from Trp111 and Leu 300 ranging from 3.7 to 4.3 Å). The carbon atom of the carboxylate group lies at 3.66 Å from the C_4 carbon of the nicotinamide moiety. As for Zopolrestat a weak hydrogen bond is placed between the 2-thioxo group of the inhibitor and Cys298 [d(C_2 = S from Cys298-SH) = 3.51 Å, angle = 125°].

The AR·Inhibitor 2 Complex. In a similar way, compound **2** shows remarkable interactions, in particular strong hydrogen bonding between the carboxylic group of the inhibitor and the hydroxyl group of Tyr48 as well as several hydrophobic interactions which hold the naphthalene ring between amino acids Trp111 and Leu300 (Figure 3). The methoxy group also demonstrates strong hydrophobic interactions with neighboring amino acids such as Trp219 and especially Leu300. The methoxy group interacts strongly with Leu300, with both Cδ and Cγ atoms of the side chain [d(O-CH$_3$−CδLeu300) = 4.09 Å and d(O-CH$_3$−CγLeu300) = 3.85 Å] and with Trp219 [d(O-CH$_3$−C_8W219) = 4.14 Å and d(O-CH$_3$−C_9W219) = 4.15 Å]. Moreover, and as previously discussed, a weak interaction exists between Cys298 and the dipolar oxo group of **2** [d(thiazolidine C_4 = O from Cys298−SH) = 3.13 Å, angle = 105°]. The carbon atom of the carboxylate group lies quite near (3.09 Å) to the C_4 carbon of the nicotinamide moiety.

Conclusion

Molecular modeling studies of our AR inhibitors together with Wilson's crystallographic results for the AR·Zopolrestat complex allow a greater understanding of the interactions involved and, hence, a better evaluation of a particular inhibitor. The structural criteria for inhibitor activity are the presence of (1) a negative charge, generally a carboxylic group able to anchor the inhibitor at the OH of Tyr48 located in the center of the anionic pocket; (2) aromatic rings capable of hydrophobic interactions with amino acids lining the enzymatic site, particularly Trp111, Leu300, and Trp219 or Trp20 as shown with inhibitors possessing only one aromatic ring;[45] (3) electronegative atoms able to form a hydrogen bond with the SH of Cys298. The stronger

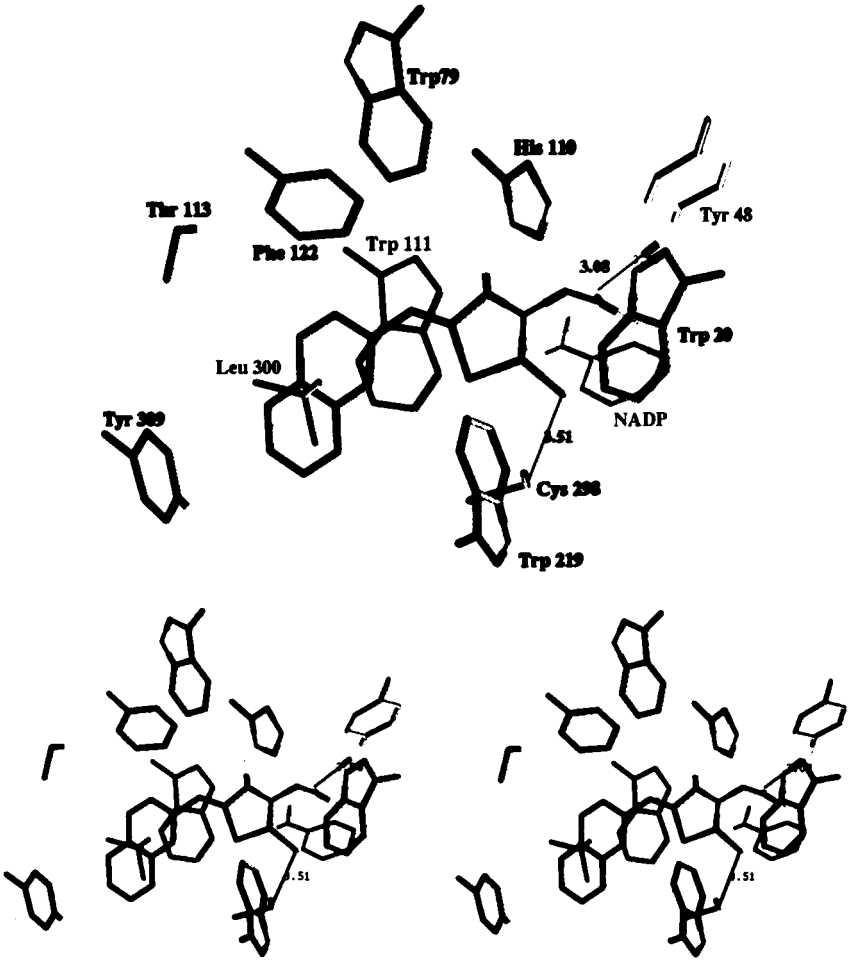

Figure 2. Inhibitor **1** docked into the aldose reductase binding pocket. The orientations of the AR amino acids (only side chains are shown) and color codes are the same as those in Figure 1. H atoms likely to make H-bonds are shown in black. H-bonds with HO-Tyr48 = 3.08 Å and with HS-Cys298 = 3.51 Å are shown (thin lines). (Top) Detailed view of AR·**1** interaction with labeled amino acids. (Bottom) Stereoview of AR·**1** interaction.

the interactions, the better the binding to AR. Several of our compounds displayed activity comparable to that Zopolrestat or Ponalrestat because they too possess the requisite features for binding to AR. In fact, although molecules **1**−**16** are less flexible than Zopolrestat, their naphthalene ring can be inserted into the groove located between Trp111 and Leu300 and form hydrophobic bonds. The flexibility of the acetic side chain allows the interaction of the carboxylate with the OH of Tyr48 by strong hydrogen bonding, thus placing the carbon atom of the carboxylate group at a favorable distance with respect to the C_4 of nicotinamide, i.e., at the site of catalytic transfer of the hydride ion. As with Zopolrestat the 2-thioxo group of compounds **1**−**8** or the 4-oxo group of compounds **9**−**16** seems to interact via hydrogen bonding with the SH of Cys298.

Molecular modeling studies clearly showed that the quality and intensity of the hydrogen bond between the carboxylic group of the inhibitor and Tyr48 are much better for Zopolrestat and **2** than for **1** (respective distances of 2.68, 2.60, and 3.08 Å). Similarly the interaction between the CO and CS groups of the inhibitors with the SH of Cys298 is much stronger for Zopolrestat and **2** than for **1**. The hydrophobic interactions between the benzothiazole ring of Zopolrestat and the naphthalene ring of **1** and **2** with Trp111 and Leu300 seem comparable. The high binding affinity of Zopolrestat for AR can be accounted for by the additional hydrogen bond between CF_3 and Thr113. Similarly the higher affinity of compound **2** compared to that of compound **1** can be accounted for by the strong hydrophobic interactions between the methoxy group of **2** and Leu300 and Trp219.

The results presented here also provide a guide for design of inhibitors with enhanced activity.

Experimental Section

Reaction progress and purity of products were checked by carrying out TLC using silica gel (Merck 60 F_{254}); the spots were located with UV light. The identity of all new compounds was confirmed by both elemental analysis (C, H, N, O, S) whose results were within ±0.4% of theoretical values and by NMR data. All melting points were determined on a Kofler bench and are uncorrected. One-dimensional and two-dimensional homonuclear or heteronuclear ^{1}H and ^{13}C NMR spectra were obtained on a Bruker AC200 FT spectrometer with TMS as an internal standard.

Synthesis of Substituted 2-Naphthaldehydes. These intermediates were synthesized by published procedures: 1-bromo-2-naphthaldehyde from 1-bromo-2-methylnaphthalene, obtained after Adams et al.,[30] according to Smith;[54] 3-bromo-2-naphthaldehyde from 3-bromo-2-methylnaphthalene−bis(hexachlorocyclopentadiene) adduct according to Smith;[54] 3-chloro-2-naphthaldehyde from 2-bromo-3-chloronaphthalene according to Lindley;[27] 1-methoxy-2-naphthaldehyde from 1-methoxynaphthalene and 3-methoxy-2-naph-

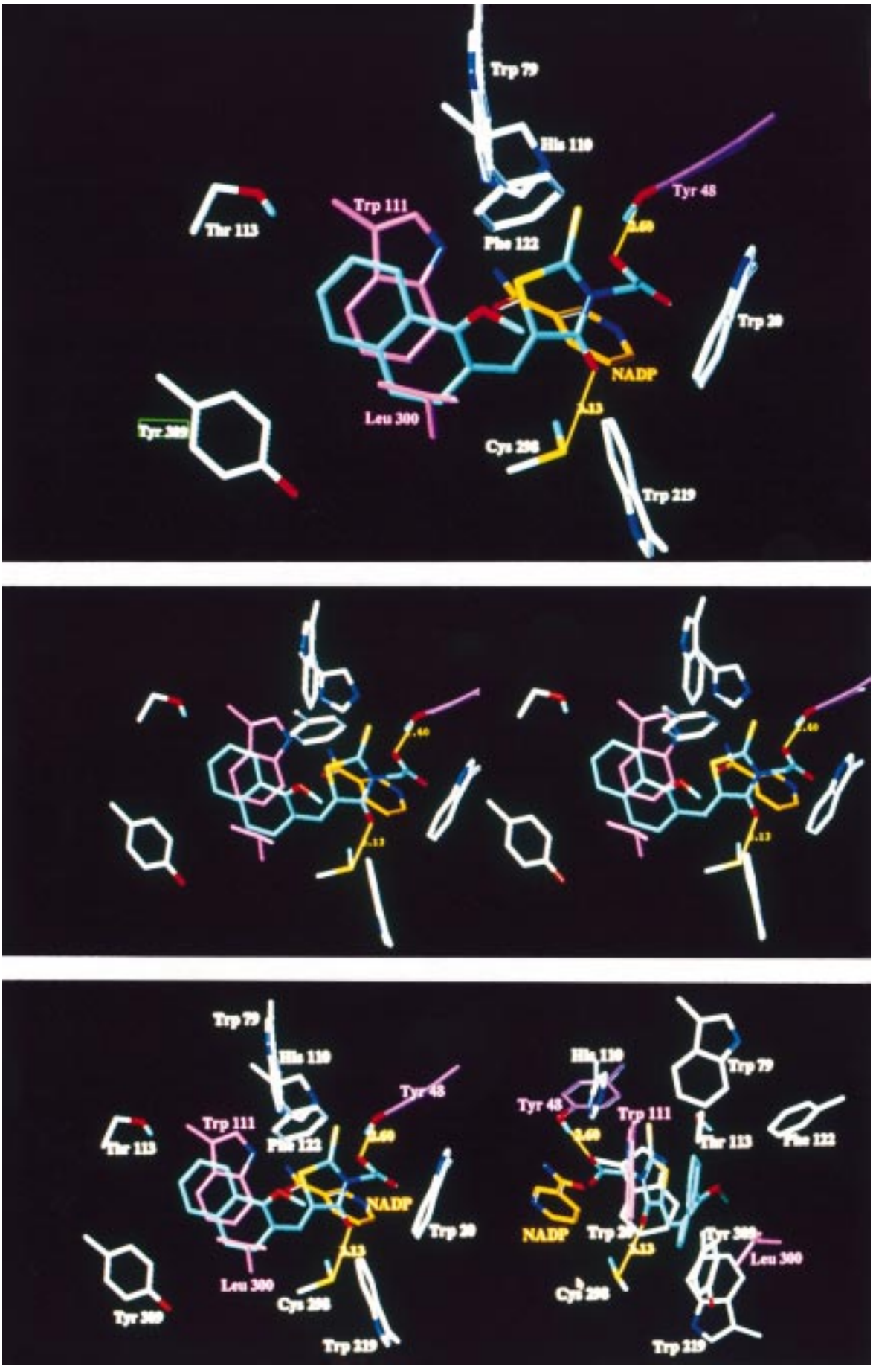
Trp 79
His 110
Tyr 48
Trp 111
Thr 113
Phe 122
Trp 20
NADP
Leu 300
Tyr 309
Cys 298
Trp 219
Trp 79
His 110
Tyr 48
Trp 111
Thr 113
Phe 122
NADP
Trp 20
Leu 300
Tyr 309
Cys 298
Trp 219
His 110
Trp 79
Tyr 48
Trp 111
Thr 113
Phe 122
NADP
Trp 20
Leu 300
Cys 298
Trp 219

Table 3. Chemical Data for Substituted 5-(2-Naphthylmethylene)-3-thiazolidineacetic Acids

		reaction conditions				
compd	substituent	temp (°C)	time (h)	purif	yield (%)	mp (°C)
		X = S, 2-Thioxo Series				
1	H	110	3.5	*a*	49.5	256−258
2	1-OCH_3	110	6	*b*	22.5	225−229
3	1-Br	110	3.5	*c*	79	265−266
4	1-NO_2	30	10	*d*	78	249−250
5	3-OCH_3	110	6	*e*	50.5	294−296
6	3-Br	110	3.5	*c*	88	269−270
7	3-Cl	110	5	*b*	55	267−269
8	6-OCH_3	110	3.5	*b*	61.5	262−264
		X = O, 2-Oxo Series				
9	H	150	23	*b*	52	251−253
10	1-OCH_3	150	13	*d*	63.5	287−292
11	1-Br	150	7.5	*f*	68.5	330−332
12[g]	1-NO_2[g]	80	2	*d*	60	288−290
13	3-OCH_3	150	13	*b*	71	278−283
14	3-Br	150	7.5	*d*	53.5	264−266
15	3-Cl	150	13	*b*	63.5	270−272
16	6-OCH_3	150	20	*f*	47	316−318

Purification: [a]crystallization from acetone; [b]washing with Et_2O; [c]crystallization from EtOH/MeOH; [d]column chromatography on silica gel with $CHCl_3$/EtOH (95:5); [e]washing with acetone; [f]crystallization from DMSO/EtOH. [g] This compound was synthesized with acetic anyhdride instead of acetic acid, in mild conditions as shown in the text.

thaldehyde from 3-methoxynaphthalene according to Narasimha;[60] 6-methoxy-2-naphthaldehyde from 6-methoxy-2-bromonaphthalene according to Eriguchi;[26] 1-nitro-2-naphthaldehyde from 1-nitronaphthalene according to Makosza.[28]

Synthesis of 2,4-Dioxo-5-(2-naphthylmethylene)-3-thiazolidineacetic Acid Derivatives. General Procedure. A solution of substituted 2-naphthaldehyde (1.03 mmol in 4 mL of acetic acid) was added to a stirred mixture of 2,4-dioxo-3-thiazolidineacetic acid (0.15 g, 0.86 mmol) and sodium acetate (0.22 g, 2.63 mmol) in 6 mL of acetic acid previously warmed for 30 min at 30 °C. The mixture was refluxed at 150 °C for various conditions of time depending on the substitution. After cooling the mixture was poured into water (30 mL) and diethyl oxide (30 mL) and stirred at room temperature for 1 h. The solid precipitate was filtered off and washed with water. The solid residue was purified by washing with cold diethyl oxide, by crystallization in the appropriate solvant or by column chromatography on silica gel with $CHCl_3$/EtOH (95:5). Details of experimental conditions are shown in Table 3.

Synthesis of 2,4-Dioxo-5-[(1-nitro-2-naphthyl)methylene]-3-thiazolidineacetic Acid. A stirred mixture of 2,4-dioxo-3-thiazolidineacetic acid (0.75 g, 4.3 mmol), sodium acetate (0.40 g, 5.0 mmol), and 1-nitro-2-naphthaldehyde (1.30 g, 6.5 mmol) in 3 mL of acetic anhydride was warmed at 80 °C for 2 h. After cooling and storing at 4 °C for 12 h, the mixture was poured into water (15 mL) and stirred for 2 h. The solid precipitate was filtered off, washed with water, and purified by column chromatography (silica gel; chloroform/ethanol, 95:5) giving 0.93 g (60% yield) of 2,4-dioxo-5-[(1-nitro-2-naphthyl)methylene]-3-thiazolidineacetic acid: mp 288−290 °C.

Synthesis of 4-Oxo-2-thioxo-5-(2-naphthylmethylene)-3-thiazolidineacetic Acid Derivatives. General Procedure. A solution of substituted 2-naphthaldehyde (4.8 mmol in 4 mL of acetic acid) was added to a stirred mixture of 4-oxo-2-thioxo-3-thiazolidineacetic acid (0.80 g, 4.2 mmol) and sodium acetate (0.86 g, 10.6 mmol) in 6 mL of acetic acid for 30 min at 30 °C. The mixture was submitted to various conditions of temperature and time, depending on the substitution. After cooling, the mixture was treated similarly as 2,4-dioxo-3-thiazolidineacetic acid derivatives. Details of experimental conditions are shown in Table 3.

Preparation of Aldose Reductase and Assay of Its Activity. The partially purified aldose reductase was prepared as described by Kador and Sharpless.[38] The beef lenses were homogenized in 96 mM phosphate buffer (pH = 6.2) at 4 °C. The homogenate was centrifuged at 15.000 t/min for 1 h at 4 °C, and the supernatant fluid was collected and could be stored at −20 °C for 1 month.

Assays of AR activity were performed spectrophotometrically as described by Kador and Sharpless[38] on a Uvikon-866 spectrophotometer at 37 °C. The reaction mixture contained 1 mL of phosphate buffer (96 mM, pH 6.2), 0.2 mL of enzyme solution, 0.4 mL of NADPH (0.18 mM), and 0.4 mL of DL-glyceraldehyde (1 mM) as a substrate. The reaction was initiated by the addition of NADPH, and the rate of NADPH oxidation was followed by recording the decrease in absorbance at 340 nm. The effects of compounds **1**−**16** on the enzyme activity were determined by adding 0.2 mL of test compound solution to the reaction mixture. The appropriate blanks to correct for nonspecific oxidation of NADPH and absorption of the reagents and of the compounds tested were prepared. Three measures of absorption were simultaneously performed for assays and blanks in an experiment. Inhibitory activities of quercitrine and Ponalrestat were tested to evaluate our experiments. Each compound was tested for four different concentrations, and five measures were performed for each concentration.

IC_{50} values were graphically measured after linear regression of inhibitory percentages expressed with logarithmic concentrations of inhibitory compounds.

Molecular Modeling Studies. All modeling procedures were performed with the Sybyl 6.1 software package[46] running on a Silicon Graphics Iris 4D-35 workstation.

Building or Retrieving Structures of Inhibitors. Structures of **1** and **2** were obtained from previous results of radiocrystallographic RX analysis[37] through atomic coordinates via Crysin tools. Structure of Zolporestat was built with the standard fragments library. Then, the corresponding anions were obtained by modification of the carboxylic group to the mesomeric carboxylate ion and addition of a formal charge −1. These anionic structures with charges of the Gasteiger−Huckel type were minimized by the Powell method[51] within Maximin 2 using the Tripos force field with the standard parameters and a value of 0.05 kcal/mol for the gradient termination cutoff. All minimizations were always run with a dielectric constant $\epsilon = 3.5$. This value was chosen because the active site pocket of AR is strongly hydrophobic.

Conformational Analysis of Inhibitors 1, 2, and Zopolrestat. We used the Gridsearch module of Sybyl. The starting conformation was, in each case, the anionic minimized structure after building (for Zopolrestat) or after setting up of crystallographic structures (for **1** and **2**). Rotatable bonds were defined: the two single bonds between heterocycle and carboxylate group for all inhibitors and the two single bonds between heterocycles for Zopolrestat (four rotatable bonds in

Figure 3. Inhibitor **2** docked into the aldose reductase binding pocket. The orientations of the AR amino acids (only side chains are shown) are the same as those in Figure 1. Color codes for heteroatoms are conventional. Carbon atoms of **2** are shown in cyan, and those of AR side-chain amino acids are shown in white except those of Trp111 and Leu300 (magenta), Tyr48 (purple), and the nicotinamide moiety (yellow). Carbon atoms of **2** are cyan. H atoms likely to make H-bonds are cyan. H-bonds with HO-Tyr48 = 2.60 Å and with HS-Cys298 = 3.13 Å are shown (thin yellow lines). (Top) Detailed view of AR·inhibitor **2** interaction with labeled amino acids. (Middle) Stereoview of AR·inhibitor **2** interaction. (Bottom) Orthographic view of AR·inhibitor **2** interaction showing $\pi-\pi$ interactions of the naphthyl moiety of **2** with Trp111 and Leu300 and tight interactions of the 1-OCH_3 substituent with Leu300 and Trp219.

all), the single bond between rings for **1** and for **2** (three rotable bonds for **1**), and in the case of **2** the bond between the OCH_3 group and the naphthyl moiety (four rotatable bonds for **2**). Angle increments usually 0−359° angle range, were 60° for Zolporestat and 30° for **1**. For **2**, angle increments were 30° relative to the first three rotatable bonds, but usual values of 0°, 90°, and 180° were set for the rotation of the fourth rotamer (relative to OCH_3 group). The minimization used in the Gridsearch method was parametrized with a maximum of 400 iterations and with other parameters set as previously for minimizations. In each case the geometries of the 12 first conformers with lower energies obtained in that way were freely optimized with Maximin 2. Then, the lowest-energy conformation resulting from this convergent procedure of optimization was chosen as the starting structure for modeling of the interaction of the inhibitor with AR.

Modeling of the Interaction of Zopolrestat and AR. 3D-Structure of AR (315 amino acids) was taken from crystallographic data of the ternary complex Aldose reductase·$NADP^+$·glucose-6-phosphate extracted from the Brookhaven Protein Data Bank (code 1ACQ)[25] within the Biopolymer module of Sybyl. The water molecules and the glucose-6-phosphate molecule were first deleted. Then $NADP^+$ atom types were corrected because atom types are typically incorrect for groups in Brookhaven files. After that Amber charges were loaded onto the protein leading to the starting conformation of AR. As usual for docking with Sybyl, the Zopolrestat and the AR starting conformations were put in two different display areas which can be superimposed to build the complex AR·Inhibitor. The inhibitor molecule was roughly put in a variety of positions allowing one of the oxygen atoms of the carboxylate group to interact with the proposed important hydroxyl group of Tyr48, at a distance of 2.6−3.1 Å and close to the plane described by this hydroxyl group, the N_ϵ of His110, and the C_4 carbon of the nicotinamide ring, while the benzenic cycle of the benzothiazole moiety of Zopolrestat was fitted into the split between Trp111 and Leu300 so that the CF_3 group of the inhibitor pointed toward the hydroxyl group of Thr113. During these trials and to adjust the position of the inhibitor, the conformation of Zopolrestat was modified by rotating within a 20° range its rotatable bonds, and the torsional angle N−Cα−Cβ−Cγ of Leu300 was modified from −133° to −153° to move slightly the Leu300 side chain away and to widen the split between Leu300 and Trp111. Finally the position of the inhibitor was refined by the Automonitor facility, and the two molecules were freezed and merged in a single area ending the construction of the candidate conformations for docking.

These conformations of the AR·inhibitor complex saved for subsequent analysis were energy-minimized by the Powell method in Maximin 2 with the Tripos force field, Gasteiger−Hückel charges, and dielectric constant $\epsilon = 3.5$, allowing 3000 iterations (the initial optimization performing a simplex minimization for 20 steps), using the Anneal function (hot region, 15 Å; interesting region, 10 Å around the inhibitor), and including termination by the energy gradient set at 0.05 kcal/mol.

Modeling of the Interaction of 1 or 2 with AR. These inhibitors were positioned as previously described for Zopolrestat for the carboxylate group, and their naphthyl ring was inserted into the split between Trp111 and Leu300. The side chain of Leu300 was moved away as in the Zopolrestat case, and adaptions of the naphthyl moiety were undertaken by slight modifications of torsional angle value of the rotatable bond between cycles. For inhibitor **2**, of the two possibilities of positioning the naphthyl ring, the one which faced the OCH_3 group and the Leu300 was clearly privileged. After a last refinement by the Automonitor facility, energy minimizations were run in the same previous conditions.

Supporting Information Available: ^1H NMR data for substituted 2-naphthaldehydes and ^1H and ^{13}C NMR data for newly synthesized compounds **1**−**16** (5 pages). Ordering information is given on any current masthead page.

References

(1) Kinoshita, J. H.; Merola, L. O.; Satoh, K.; Dikmak, E. Osmotic changes caused by the accumulation of dulcitol in the lenses of rats fed with galactose. *Nature* **1962**, *194*, 1085−1087.

(2) Gabbay, K. H.; O'Sullivan, J. B. The sorbitol pathway: enzyme localization and content in normal and diabetic nerve and cord. *Diabetes* **1968**, *17*, 239−243.

(3) Kinoshita, J. H. Cataracts in galactosemia. *Invest. Ophthalmol.* **1965,** *4* (5), 786−799.

(4) Kinoshita, J. H.; Dvornik, D.; Kraml, M.; Gabbay, K. H. The effects of an aldose reductase inhibitor on galactose-exposed rabbit lens. *Biochim. Biophys. Acta* **1968**, *158*, 472−475.

(5) Gabbay, K. H. Hyperglycemia, polyol metabolism and complications of diabetes mellitus. *Annu. Rev. Med.* **1975**, *26*, 521−536.

(6) Dvornik, D. Chronic complications of diabetes. *Annu. Rep. Med. Chem.* **1978**, *13*, 159−166.

(7) Robison, W. G.; Kador, P. F.; Kinoshita, J. H. Retinal capillaries: basement membrane thickening by galactosemia prevented with aldose reductase inhibitor. *Science* **1983**, *221*, 1177−1179.

(8) Lipinski, C. A.; Hutson, N. J. Aldose reductase inhibitors as a new approach to the treatment of diabetic complications. *Annu. Rep. Med. Chem.* **1984**, *19*, 169−177.

(9) Cogan, D. G.; Kinoshita, J. H.; Kador, P. F.; Robison, W. G.; Datiles, M. B.; Cobo, L. M.; Kupfer, C. NIH conference. Aldose reductase and complications of diabetes. *Ann. Intern. Med.* **1984**, *101* (1), 82−91.

(10) Kador, P. F.; Robison, W. G.; Kinoshita, J. H. The pharmacology of aldose reductase inhibitors. *Annu. Rev. Pharmacol. Toxicol.* **1985**, *25*, 691−714.

(11) Tomlinson, D. R.; Willars, G. B.; Carrington, A. L. Aldose reductase inhibitors and diabetic complications. *Pharmacol. Ther.* **1992**, *54* (2), 151−194.

(12) Kador, P. F.; Kinoshita, J. H.; Sharpless, N. E. Aldose-reductase inhibitors: a new class of agents for the pharmacological control of certain diabetic complications. *J. Med. Chem.* **1985**, *28*, 841−849.

(13) Humber, L. G. The medicinal chemistry of aldose reductase inhibitors. *Prog. Med. Chem.* **1987**, *24*, 299−343.

(14) Sarges, R. Aldose reductase inhibitors. In *Trends in Medicinal Chemistry. Ninth Symposium*; Mutschler, E., Winterfeldt, T. E., Eds.; VCH: Basel, 1987; pp 551−564.

(15) Kador, P. F. The role of aldose reductase in the development of diabetic complications. *Med. Res. Rev.* **1988**, *8* (3), 325−352.

(16) Larson, E. R.; Lipinski, C. A.; Sarges, R. Medicinal chemistry of aldose reductase inhibitors. *Med. Res. Rev.* **1988**, *8* (2), 159−186.

(17) Sarges, R. Aldose reductase inhibitors: structure−activity relationships and therapeutic potential. In *Advances in Drug Research*; Testa, B., Ed.; Academic Press Ltd.: London, 1989; Vol. 18, p 139.

(18) Sarges, R.; Oates, P. J. Aldose reductase inhibitors: recent developments. *Prog. Drug Res.* **1993**, *40*, 99−161.

(19) Kador, P. F.; Sharpless, N. E. Pharmacophore requirements of the aldose reductase inhibitor site. *Mol. Pharmacol.* **1983**, *24* (3), 521−531.

(20) Chazeau, V.; Cussac, M.; Boucherle, A. Study of 5-arylidene-2-thiohydantoins with potential immunomodulating and anticancer activities. *Eur. J. Med. Chem.* **1992**, *27* (6), 615−625.

(21) Rondeau, J. M.; Tete-Favier, F.; Podjarny, A.; Reymann, J. M.; Barth, P.; Biellmann, J. F.; Moras, D. Novel NADPH-binding domain revealed by the crystal structure of aldose reductase. *Nature* **1992**, *355*, 469−472.

(22) Wilson, D. K.; Bohren, K. M.; Gabbay, K. H.; Quiocho, F. A. An unlikely sugar substrate site in the 1.65 Å structure of the human aldose reductase holoenzyme implicated in diabetic complications. *Science* **1992**, *257*, 81−84.

(23) Borhani, D. W.; Harter, T. M.; Petrash, J. M. The crystal structure of the aldose reductase•NADPH binary complex. *J. Biol. Chem.* **1992**, *267* (34), 24841−24847.

(24) Wilson, D. K.; Tarle, I.; Petrash, J. M.; Quiocho, F. A. Refined 1.8 Å structure of human aldose reductase complexed with the potent inhibitor zopolrestat. *Proc. Natl. Acad. Sci. U.S.A.* **1993**, *90*, 9847−9851.

(25) Harrison, D. H.; Bohren, K. M.; Ringe, D.; Petsko, G. A.; Gabbay, K. H. An anion binding site in human aldose reductase: mechanistic implications for the binding of citrate, cacodylate and glucose 6-phosphate. *Biochemistry* **1994**, *33* (8), 2011−2020.

(26) Eriguchi, A.; Takegoshi, T. Studies on hypolipidemic agents. I. Synthesis of 1,3-dioxolanes and 1,3-dioxanes. *Chem. Pharm. Bull.* **1982**, *30*, 428−439.

(27) Lindley, W. A.; McDowell, D. W. H. Keto−enol tautomerism in the thiophene analogues of naphthacen-5-one. *J. Org. Chem.* **1982**, *47*, 705−709.

(28) Makosza, M.; Owczarczyk, Z. Dihalomethylation of nitroarenes via Vicarious nucleophilic substitution of hydrogen with trihalomethyl carbanions. *J. Org. Chem.* **1989**, *54*, 5094−5100.

(29) Corey, E. J.; Suggs, J. W. Pyridinium chlorochromate. An efficient reagent for oxidation of primary and secondary alcohols to carbonyl compounds. *Tetrahedron Lett.* **1975**, *31*, 2647−2650.
(30) Adams, R.; Binder, L. O. Restricted rotation in aryl olefins. III. Preparation and resolution of β-chloro-β-(2-methyl-1-naphthyl)-acrylic acids. *J. Am. Chem. Soc.* **1941**, *63*, 2773−2775.
(31) Danish, A. A.; Silverman, M.; Tajima, Y. A. Dienophilic reactions of aromatic double bonds in the synthesis of β-substituted naphthalenes. *J. Am. Chem. Soc.* **1954**, *76*, 6144−6150.
(32) Fresneau, P.; Thomasson, F.; Morand, J. M.; Cussac, M. 5-Aryl-methylene thiazolidine derivatives: ^{1}H and ^{13}C NMR chemical shifts assigments and determination of the stereochemistry by coupling constant measuring with coupled ^{13}C NMR. *Spectrochim. Acta* **1998**, in press.
(33) Katritski, A. R.; Hitchings, G. J.; King, R. W.; Zhu, D. W. ^{1}H and ^{13}C nuclear magnetic resonance studies of ethenyl-substituted benzenoid aromatic compounds. *Magn. Res. Chem.* **1991**, *29* (1), 2−8.
(34) Breitmaier, R. M.; Bassler G. C. *Carbon 13 NMR Spectroscopy*, 3rd ed.; VCH: Weinheim, 1987; pp 1−515.
(35) Voegeli, U.; Von Philipsborn, W.; Nagarajan, K.; Nair, M. D. Structure of addition products of acetylenedicarboxylic acid esters with various dinucleophiles. An application of C, H-spin-coupling constants. *Helv. Chim. Acta* **1978**, *61* (2), 607−617.
(36) Ishida, T.; In, Y.; Inoue, M.; Ueno, Y.; Tanaka, C.; Hamanaka, N. Structural elucidation of epalrestat (ONO-2235), a potent aldose reductase inhibitor, and isomerization of its double bonds. *Tetrahedron Lett.* **1989**, *30* (8), 959−962.
(37) Tranqui, D.; Fresneau, P.; Cussac, M. Crystal structure of *(Z)*-5-(1-methoxy-2-naphthylmethylidene)-4-oxo-2-thioxothiazolidine-3-yl acetic acid. *Acta Crystallogr.* **1998**, *C54*, 1152−1154.
(38) Kador, P. F.; Sharpless, N. E. Structure−activity studies of aldose reductase inhibitors containing the 4-oxo-4-*H*-chromen ring system. *Biophys. Chem.* **1978**, *8* (1), 81−85.
(39) Ward, W. H. J.; Sennitt, C. M.; Ross, H.; Dingle, A.; Timms, D.; Mirrlees, D. J.; Tuffin, D. P. Ponalrestat: a potent and specific inhibition of aldose reductase. *Biochem. Pharmacol.* **1990**, *39* (2), 337−346.
(40) Brittain, D. R. In *Proceedings of the Third SCI-RSC Medicinal Chemistry Symposium*; Lambert, R. W., Ed.; Royal Society of Chemistry: London, 1986; pp 210−240.
(41) Mylari, B. L.; Larson, E. R.; Beyer, T. A.; Zembrowski, W. J.; Aldinger, C. E.; Dee, M. F.; Siegel, T. W.; Singleton, D. H. Novel, potent aldose reductase inhibitors: 3,4-dihydro-4-oxo-3-[(5-(trifluoromethyl)-2-benzothiazolyl)-methyl]-1-phthalazineacetic acid (zopolrestat) and congeners. *J. Med. Chem.* **1991**, *34*, 108−122.
(42) Terashima, H.; Hama, K.; Yamamoto, R.; Tsuboshima, M.; Kikkawa, R.; Hatanaka, I.; Shigeta, Y. Effects of a new aldose reductase inhibitor on various tissues in vitro. *J. Pharmacol. Exp. Ther.* **1984,** *229* (1), 226−230.
(43) Sestanj, K.; Bellini, F.; Fung, S.; Abraham, N.; Treasurywala, A.; Humber, L.; Simard-Duquesne, N. S.; Dvornik, D. N-[5-(trifluoromethyl)-6-methoxy-1-naphthalenyl]thioxomethyl]-*N*-methylglycine (Tolrestat), a potent, orally, active aldose-reductase inhibitor. *J. Med. Chem.* **1984**, *27*, 255−256.
(44) Sarges, R.; Peterson, M. J. Sorbinil: a member of the novel class of spirohydantoin aldose reductase inhibitors. *Metabolism* **1986**, *35* (Suppl. 1), 101−104.
(45) Ehrig, T.; Böhren, K. M.; Prendergast, F. G.; Gabbay, K. H. Mechanism of aldose reductase inhibition: Binding of $NADP^{+}$/NADPH and alrestatin-like inhibitors. *Biochemistry* **1994**, *33*, 7157−7165.
(46) SYBYL 6.1; 1994; Tripos Associates, 1699 S. Hanley Rd, Suite 303, St. Louis, MO 63144.
(47) Tarle, I.; Borhani, D. W.; Wilson, D. K.; Quiocho, F. A.; Petrash, J. M. Probing the active site of human aldose reductase. Site-directed mutagenesis of Asp43, Tyr48, Lys77, and His110. *J. Biol. Chem.* **1993**, *268* (34), 25687−25693.
(48) Börhen, K. M.; Grimwasch, C. E.; Lai, C. J.; Harrison, D. H.; Ringe, D.; Petsko, G. A.; Gabbay, K. H. Tyrosine-48 is the proton donor and histidine-110 directs substrate stereochemical selectivity in the reduction of human aldose reductase: enzyme kinetics and crystal structure of the Y48H mutant enzyme. *Biochemistry* **1994**, *33*, 2021−2032.
(49) Carper, D. A.; Hohman, T. C.; Old, S. E. Residues affecting the catalysis and inhibition of rat lens aldose reductase. *Biochim. Biophys. Acta* **1995**, *1246*, 67−73.
(50) Bhatnagar, A.; Liu, S. Q.; Ueno, N.; Chakrabarti, B.; Srivastava, S. K. Human placental aldose reductase: role of Cys298 in substrate and inhibitor binding. *Biochim. Biophys. Acta* **1994**, *1205* (2), 207−214.
(51) Powell, M. J. D. Restart procedures for the conjugate gradient method. *Mathematical Programming* **1977**, *12*, 241−254.
(52) Morjana, N. A.; Flynn, T. G. Aldose reductase from human psoas muscle: purification, substrate specificity, immunological characterization, and effect drugs and inhibitors. *J. Biol. Chem.* **1989**, *264* (5), 2906−2911.
(53) Wermuth, B.; Monder, C. Aldose and aldehyde reductase exhibit isocorticosteroid reductase activity. *Eur. J. Biochem.* **1983**, *131* (2), 423−426.
(54) Smith, J. G.; Dibble, P. W.; Sandborn, R. E. The preparation and reactions of Naphtho[1,2-c]furans and naphtho[2,3-c]furans. *J. Org. Chem.* **1986**, *51*, 3762−3768.
(55) Look, M.; Padgett, W. M.; Hyman, J.; Fenyes, J. G. E.; Lee, H. P. C. 3-Hydroxy-2-naphthoic acid. *Chem. Abstr.* **1965**, *62*^{P}, 503^{e}.
(56) Narasimhan, N. S.; Mali, R. S. Synthetic application of lithiation reactions − VII. New synthesis of linear and angular Naphthofurans and Benzocoumarins. *Tetrahedron* **1975**, *31*, 1005−1009.

JM9801399